Published in final edited form as:

Oncogene. 2019 January ; 38(1): 47–59. doi:10.1038/s41388-018-0436-4.

Mouse ER+/*PIK3CA*^{H1047R} breast cancers caused by exogenous estrogen are heterogeneously dependent on estrogen and undergo BIM-dependent apoptosis with BH3 and PI3K agents

Elias E. Stratikopoulos[1], **Nicole Kiess**[1], **Matthias Szabolcs**[2], **Sarah Pegno**[1], **Cheung Kakit**[1], **Xuewei Wu**[1], **Poulikos I. Poulikakos**[1], **Pamela Cheung**[1], **Hank Schmidt**[3], and **Ramon Parsons**[1]

[1]Department of Oncological Sciences, Tisch Cancer Institute, Icahn School of Medicine at Mount Sinai, New York, NY 10029, USA

[2]Department of Pathology, Columbia University Medical Center, New York, NY 10032, USA

[3]Department of Surgery, Tisch Cancer Institute, Icahn School of Medicine at Mount Sinai, New York, NY 10029, USA

Abstract

Estrogen dependence is major driver of ER + breast cancer, which is associated with PI3K mutation. PI3K inhibition (PI3Ki) can restore dependence on ER signaling for some hormone therapy-resistant ER + breast cancers, but is ineffective in others. Here we show that short-term supplementation with estrogen strongly enhanced *Pik3caH1047R*-induced mammary tumorigenesis in mice that resulted exclusively in ER + tumors, demonstrating the cooperation of the hormone and the oncogene in tumor development. Similar to human ER + breast cancers that are endocrine-dependent or endocrine-independent at diagnosis, tumor lines from this model retained ER expression but were sensitive or resistant to hormonal therapies. PI3Ki did not induce cell death but did cause upregulation of the pro-apoptotic gene BIM. BH3 mimetics or PI3Ki were unable to restore hormone sensitivity in several resistant mouse and human tumor lines. Importantly however, combination of PI3Ki and BH3 mimetics had a profound, BIM-dependent cytotoxic effect in PIK3CA-mutant cancer cells while sparing normal cells. We propose that addition of BH3 mimetics offers a therapeutic strategy to markedly improve the cytotoxic activity of PI3Ki in hormonal therapy-resistant and ER-independent PIK3CA-mutant breast cancer.

Introduction

Luminal (HER2^{-}negative) breast cancers that are characterized by expression of estrogen receptor α (ER) account for 65–70% of breast cancers and are usually dependent on estrogen for their growth. Several antiestrogen therapeutic options are currently available to treat women with this disease including aromatase inhibitors (AIs), which inhibit the

*Ramon Parsons ramon.parsons@mssm.edu.

Electronic supplementary material The online version of this article (https://doi.org/10.1038/s41388-018-0436-4) contains supplementary material, which is available to authorized users.

Conflict of interest The authors declare that they have no conflict of interest.

synthesis of estrogen, selective ER modulators such as tamoxifen, and selective ER degraders like fulvestrant. These agents have revolutionized the treatment of breast cancer patients by reducing the relative risk of recurrence by approximately 40% in early-stage disease [1] and improving the outcome in those with advanced disease [2]. Despite this efficacy, prognosis remains poor for many patients due to intrinsic or acquired resistance to endocrine therapy. Ligand-independent activation of ER signaling through mutations in *ESR1,* the gene encoding the ER, or activation of growth factor receptor pathways can drive resistance to endocrine therapy in some cases [3–5]. However, loss of ER expression, though uncommon, can also induce resistance to endocrine therapy and conversion to an endocrine-insensitive phenotype [6].

In search of combinatorial partners to battle resistance to hormonal therapy, the PI3K pathway represents an attractive target as it is frequently activated in breast cancer including the ER-positive (ER^+) and ER^+-endocrine therapy-resistant subgroups [7, 8]. In particular, hot-spot mutations in *PIK3CA,* the gene encoding the catalytic subunit of PI3Kα, constitute one of the major routes of activation of the PI3K signal and have been shown to correlate with ER^+ status [9]. Interestingly, numerous preclinical studies have identified the PI3K pathway as a point of sensitivity in long-term estrogen-deprived ER^+ cells [10–12]. Targeting PI3K in ER^+ cells has also been shown to enhance ER transcriptional activity and in some instances restore sensitivity to endocrine therapy [13–16].

In light of these findings, results from two randomized trials, TAMRAD [17] and BOLERO-2 [18], have shown that addition of everolimus (a small molecule inhibitor of TORC1, a downstream effector of PBK/AKT) to anti-estrogen therapy improved progression-free survival in women with advanced breast cancer, leading to the approval of this treatment by the Food and Drug Administration (FDA). Although results from trials with endocrine therapy in combination with inhibitors targeting all PI3K isoforms (pan-PI3K) have been discouraging due to toxicity and limited efficacy [19–21], results using inhibitors that show a greater selectivity against PIK3CA-mutant isoforms such as alpelisib (BYL719), a PI3Kα-selective inhibitor [22–24], and taselisib (GDC-0032), a PBKβ-sparing inhibitor [25–27], are highly anticipated in the field. Nevertheless, preclinical studies and results from early phase clinical trials suggest that not all patients, even those with PIK3CA-mutant cancers, will benefit equally from PI3K-targeted therapies and alternative rational combination strategies remain underexplored.

In this study, we use a *Pik3ca*^{H1047R} knockin mouse and exogenous administration of estrogen to model ER +/PIK3CA-mutant breast cancer and explore treatment options for hormone therapy-resistant tumors. This approach had led to the identification of BIM induction after treatment with BYL719 as an indicator of the therapeutic benefit of BH3 mimetics, which can enhance the cytotoxic activity of PI3K inhibition in PIK3CA-mutant breast cancers irrespective of their ER status.

Results

Estrogen supplementation enhances Pik3ca^{H1047R}-induced mammary tumorigenesis in mice

To examine the oncogenic effects of deregulated ER activity on mammary tumorigenesis driven by the H1047R hot-spot *Pik3ca* mutation in vivo, we first crossed mice carrying a dormant H1047R *Pik3ca* mutation [28] with *Wap*^{Cre} drivers [29] to generate a cohort of experimental *Pik3ca*^{H1047R}/*Wap*^{Cre} (*Pik3ca*^{H1047R}) female mice. In these mice, activation of the mutant p110α is dependent on expression of a Cre-recombinase that has been inserted by knockin to the *Wap* gene (encoding the milk whey acidic protein) and is restricted to alveolar and ductal mammary epithelial cells during late pregnancy and throughout lactation. *Pik3ca*^{H1047R} females were then mated to induce Cre expression, and 17β-estradiol (E2) 90-day release pellets were implanted 2–3 weeks postpartum in a subset of the *Pik3ca*^{H1047R} animals (*Pik3ca*^{H1047R} + E2). Females carrying only the *Wap*^{Cre} transgene served as controls. Mice underwent multiple pregnancies and were monitored for mammary tumor formation by palpation once a week until they became 1.5 years old.

All of the control *Wap*^{Cre}-only mice remained tumor-free, whereas mammary tumors developed in *Pik3ca*^{H1047R} + E2 mice around a year post first parturition (T_{50} = 353) and at complete penetrance (9/9 animals) (Fig. 1a). Tumors in these animals frequently involved more than one mammary gland and would often grow to 100–200 mm^3 within one month after initial detection by palpation (Supplementary Figure 1A). On the contrary, mammary tumor development in *Pik3ca*^{H1047R} animals without exogenous estrogen manifested after a longer latency (T_{50} = 471 days after the first parturition) and with a lower incidence (13/19 animals). These mammary tumors were small, not exceeding 32 mm^3 in volume, and solitary in all but five animals (Supplementary Figure 1A).

In *Pik3ca*^{H1047R} + E2 animals, 56% of the invasive mammary carcinomas involved a glandular component intermixed with squamous cells (adenosquamous carcinomas) and 42% of the tumors were identified as adenocarcinomas with no other histology (Supplementary Figure 1B and C). In *Pik3ca*^{H1047R} animals without exogenous estrogen, the majority of the tumors (76%) were squamous cell carcinomas (SCC) with coherent, large polygonal cells infiltrating the adjacent stroma in small irregular nests and a glandular component was identified in only 18% of these (Supplementary Figure 1B and C). Keratinization was commonly noted in SCC, which was also seen growing along preformed breast ducts adjacent to the invasive carcinoma consistent with an in-situ component. A single case of a carcinosacroma was observed in each cohort.

Of note, all of the tumors in *Pik3ca*^{H1047R} + E2 animals were strongly positive for ER by IHC, whereas in animals without E2 pellets both the squamous and glandular components were predominantly negative for ER, although occasional cells displayed weak labeling (Fig. 1b, c and Supplementary Figure 1C and Supplementary Table 1). Regardless of estrogen supplementation, as expected, squamous cells were consistently positive for basal cytokeratins 5 and 14 and negative for the luminal cytokeratin 18, and cells forming the glandular component were predominantly negative for cytokeratin 5 and positive for cytokeratins 14 and 18 (Supplementary Figure 1C and Supplementary Table 1). Collectively,

these data suggest that estrogen can cooperate with the H1047R *Pik3ca* mutation in mammary tumorigenesis and drive the formation of exclusively ER^+ tumors that show an enriched glandular differentiation.

Generation of ER^+/$Pik3ca^{H1047R}$ mouse cancer cell lines

Implantation of E2 pellets into lactating $Pik3ca^{H1044R}$ female mice had a dramatic impact on the ER status of the mammary tumors, even though tumors in these animals are identified several months after the releasing action of the pellets has ceased. To better characterize these tumors and test their response to hormonal therapies we generated three cell lines from different tumor-bearing mice. These cell lines, namely FR-1, FR-2, and FS-1, consisted of both basal and luminal epithelial cells and expressed the oncogenic H1047R *Pik3ca* mutation (Fig. 2a, b and Supplementary Figure 2A).

To determine whether these cell lines are dependent on estrogen for growth we grew them in steroid-free medium for several days and then treated with E2 and monitored cell growth using a live cell imaging system. MCF7 and T47D ER^+ human breast cancer cells served as positive controls. Notably, FR-1 and FR-2 cells grew equally well with or without E2, suggesting that they are not dependent on estrogen for their growth (Supplementary Figure 2B), whereas FS-1 cells did not grow in steroid-free medium. FR-1 cells were also able to form tumors in wild-type C57BL/6J mice without the need to implant E2 pellets (Supplementary Figure 2C). As expected, MCF7 and T47D cells were growth inhibited in the absence of steroids and were highly responsive to stimulation with E2 (Supplementary Figure 2B).

We also examined the response of these mouse cell lines to different hormonal therapies using ER^+ (MCF7 and T47D) and ER-(MDA-MB-468) cells as positive and negative controls, respectively. FR-1, FR-2 and MDA-MB-468 cells were resistant to treatment with 4-OH tamoxifen as well as the ER antagonist fulvestrant despite downregulation of ER (Fig. 2c), whereas FS-1, MCF7, and T47D cells were highly sensitive to both treatments (Fig. 2d and Supplementary Figure 3). Therefore, similar to human ER^+ primary breast cancers, this ER^+;Pik3ca-mutant mouse model develops tumors that can be either sensitive to hormonal therapies or intrinsically resistant.

PI3Kα inhibition fails to resensitize ER^+ cells to fulvestrant and trigger apoptosis despite induction of BIM

PI3K inhibition has been previously shown to increase ER transcriptional activity and dependence, resulting in resistance to PI3K inhibition as a single agent in some hormone-receptor-positive breast cancers [11]. Indeed, treatment with the highly selective PI3Kα inhibitor alpelisib (BYL719) resulted in an increase of both mRNA and protein levels of ER in FR-1 but not in FR-2 and FS-1 cells (Fig. 3a and Supplementary Figure 4A). However, addition of fulves-trant provided no benefit to treatment with BYL719, suggesting that this combination may not be effective in certain ER^+ breast cancers that no longer rely on estrogen for their growth (Fig. 3b and Supplementary Figure 4B).

The PI3K pathway is a critical mediator of cell survival that inhibits apoptosis signals, and inhibition of the PI3K signal should create a signaling state that is permissive for apoptotic

signaling. Although treatment with BYL719 modestly inhibited cell growth, it uniformly failed to induce cell death in all three mouse cell line models even in the presence of fulvestrant (Fig. 3c and Supplementary Figure 4C). Given the critical role of the BCL-2 family of pro- and anti-apoptotic proteins in regulating cell survival, we sought to examine the effects of PI3Kα inhibition on some of these genes. Unexpectedly, a significant increase of the pro-apoptotic BCL-2 family member *Bim* mRNA was the only consistent change in response to treatment with BYL719 (Fig. 3d and Supplementary Figure 4D), and Bim protein levels were also increased in a dose and time-dependent manner in FR-1 cells (Fig. 3e, f). Interestingly, Bim upre-gulation was also documented in DMSO-treated samples overtime, most likely as a result of gradual growth factor and nutrient deprivation, which is known to induce expression of Bim [30]. Nevertheless, Bim induction in BYL719-treated cells was markedly higher that what was observed in DMSO-only cells (Fig. 3f).

To further establish the relevance of our findings with the human disease, MCF7 and T47D cells underwent long-term treatment with fulvestrant and resistant clones were generated that had either lost expression of ER (MCF7-FR) or ER was no longer degraded by fulvestrant (T47D-FR). Similarly to what we observed in the mouse cell line models, PI3Kα inhibition provided little benefit to treatment with fulvestrant and failed to induce cell death despite upregulation of the mediator of cell death BIM in both MCF7-FR and T47D-FR cells (Supplementary Figure 5). Taken together, these results indicate that PI3Kα inhibition does not restore sensitivity to fulvestrant in certain ER^+ cells that have developed resistance to this ER antagonist, and also fails to induce apoptosis despite the upregulation of the mediator of cell death BIM.

BH3 mimetics enhance the efficacy of PI3Kα inhibition

Induction of apoptosis is critical for tumor regression in vivo and a diminished apoptotic response could limit the efficacy of PI3Kα targeted therapies. Given that BIM can be bound and presumably neutralized by anti-apoptotic BCL-2 family members, we hypothesized that the use of BH3 mimetics, a class of drugs that bind to and inhibit these proteins, might release BIM from its inhibitory partners and allow it to mediate apoptosis. To test this we used navitoclax (ABT263), a BH3 mimetic that directly binds to BCL-XL, BCL-2, and BCL-W and prevents them from binding to and inhibiting BIM. Mouse and human cells were treated with fulvestrant, BYL719, ABT263, and their combinations and the effects on cell growth and death were measured. Interestingly, cells did not respond to ABT263 alone, but the BH3 mimetic was highly effective at inhibiting cell growth and inducing cell death when added to the fulvestrant/BYL719 dual therapy (Fig. 4a–c and Supplementary Figures 5A–C and 6). Notably addition of fulvestrant did not enhance BYL719/ABT263-induced cell death (Fig. 4b and Supplementary Figures 5C and 6C), suggesting that treatment with fulvestrant may be dispensable in ER^+ tumors that do not rely on estrogen for their growth.

We then asked which anti-apoptotic members of the BCL-2 family can mediate the antitumor effects of ABT263. To this end, we compared the cell growth inhibitory action of BH3 mimetics that are selective against BCL-2, BCL-XL, or MCL-1 (venetoclax/ABT199, A1155463 and A1210477, respectively) with that of ABT263 in cells that were treated with fulvestrant/BYL719. Inhibition of any individual anti-apoptotic member of the BCL-2

family was able to either partially (FR-1) or fully (MCF7-FR and T47D-FR) recapitulate the growth inhibitory effect of ABT263 (Fig. 4d and Supplementary Figure 7), suggesting that multiple anti-apoptotic BCL-2 family members are involved in the evasion of cell death after treatment with BYL719.

Of note BIM, unlike more selective BH3-only proteins (such as BAD and NOXA), can bind with high affinity to all anti-apoptotic BCL-2 family members [31], which could explain why BH3 mimetics with different selectivity are all effective to some extent in combination with PI3Kα inhibition. To test the hypothesis that Bim induction is important in mediating the effects of ABT263, Bim was stably knocked down using shRNA (Fig. 4e), and the effects of BYL719 and ABT263 on growth were examined in FR-1 cells. As expected, treatment with ABT263 was unable to increase the efficacy of BYL719 in FR-1 cells transduced with a hairpin to *Bim,* but persisted similarly to parental cells in control knockdown cells (Fig. 4f).

BH3 mimetics and PI3Kα inhibition are efficacious irrespective of ER status

The enhanced efficacy of PI3Kα inhibition and BH3 mimetics in cells that are resistant to hormonal therapy suggested that this combination might also be beneficial in tumors that harbor mutations in the PI3K pathway irrespective of their hormonal status. To address this possibility we extended our study in a panel of *PIK3CA-mutant,* ER^+ (MCF7, T47D, BT474) or ER^- (HCC202, MDA-MB-453, and SUM159) human breast cancer cell lines and assessed the effects of ABT263 and BYL719 both alone and in combination. Treatment with BYL719 failed to induce apoptosis beyond control levels in most cell lines, even though it consistently resulted in upregulation of *BIM* mRNA. However, the addition of ABT263 was able to significantly increase the cytotoxic and growth inhibitory effects of BYL719, albeit to different extents (Fig. 5a–c). Several anti-apoptotic BCL-2 family members were induced after treatment with BYL719 in all cell lines (Supplementary Figure 8), suggesting that a more complex regulation of the BCL-2 family that alters the balance of anti- and pro-apoptotic members might be responsible for the enhanced efficacy of the combination treatment.

We next asked whether the BYL719/ABT263 combination would also be efficacious in cancers with wild-type PIK3CA. Similarly to PIK3CA-mutant cells, treatment with BYL719 failed to induce cell death in three PIK3CA wild-type breast cancer cells but in this case it was not accompanied by upregulation of *BIM* (Fig. 5a, b). Concordantly, addition of ABT263 did not significantly increase the cytotoxic and growth inhibitory activity of BYL719 in these cells (Fig. 5a, c), suggesting that this combination might not be suitable for patients with wild-type PIK3CA tumors.

To further assess the clinical relevance of our findings, we tested the effects of BYL719, ABT263, and their combination on early passage tumor-derived cultures from three ER^+/$HER2^-$ breast cancer patients who had not received any prior treatment, two of which (patients 2 and 3) had hotspot mutations in exon 9 of *PIK3CA* by RNA-seq. We confirmed the epithelial nature of the cells with immune-fluorescence (IF) for cytokeratins and activation of the PI3K pathway (Supplementary Figure 9A and B). In agreement with our previous results, treatment with BYL719 or ABT263 alone failed to induce cell death

beyond background levels (DMSO-treated cells) despite induction of BIM as a result of treatment with BYL-719 (Fig. 5d, e). However, combined treatment was superior at tumor cell killing, and this was accompanied by enhanced inhibition of cell growth, albeit to different degrees (Fig. 5e,f). Interestingly, induction of BIM protein and mRNA levels after treatment with BYL719 was highest in tumor-derived cultures with the highest baseline activation of the PI3K pathway as measured by phosphorylation of AKT (Supplementary Figure 9B), suggesting that BIM is directly regulated by PI3K activity. Moreover, these cells did not show any nuclear staining for ER by IF (Supplementary Figure 9A), which could be due to either the low percentage of ER^+ cells in these tumor biopsies (8−12%) or the loss of expression upon in vitro culturing. As a result, treatment with fulvestrant did not further improve the effects of the BYL719/ABT263 combination treatment (Supplementary Figure 9C).

Any drug combination that induces a strong cytotoxic effect in cancer cells will not be clinically effective if it has the same effects in nonmalignant cells. To address this possibility, we compared the responses of tumor-derived and normal cells from the same patients to the different drug combinations as measured by the inclusion of DRAQ7, a fluorescent dye that stains dead cells. Importantly, BYL719/ABT263 treatment with or without fulvestrant was more effective at killing tumor cells compared to breast epithelial cells derived from the same patient (Supplementary Figure 9D), suggesting that this drug combination could have tolerable toxicities in cancer patients.

ABT263 enhances the antitumor activity of BYL719 in vivo

We next assessed the toxicity and efficacy of the combined BYL719/ABT263 treatment in vivo. In the FR-1 allograft model, BYL719 (50 mg/kg/d) or ABT263 (60 mg/kg/d) alone showed modest effects on cell growth, whereas the combination almost completely blocked growth of these tumors (Fig. 6a). Pharmacodynamic studies confirmed that BYL719 blocked activation of the PI3K pathway as measured by AKT phosphorylation. Moreover, cleaved caspase-3, a marker of apoptosis, was markedly increased following combination treatment, consistent with our in vitro studies (Fig. 6b). No overt toxicities were observed in the tumor-bearing mice treated with the combination for 12 days (Supplementary Figure 10A). Similar results were obtained with the MCF7-FR xenograft model treated with the same doses for 21 days (Supplementary Figures 10B–D). Collectively, our in vitro and in vivo data support a model where inhibition of PI3Kα can result in the induction of the pro-apoptotic BCL-2 family member BIM in *PIK3CA*- mutant tumors. However, this fails to induce apoptosis as BIM induction may be neutralized by the available pool of its anti-apoptotic binding partners. Importantly, this can be reverted by the addition of a BH3 mimetic, which then allows BIM to exert its pro-apoptotic function (Fig. 6c).

Discussion

Immortalized ER^+ human breast cancer cell lines have been the tool of choice for studying the biology of this particular subtype as most tumors arising in genetically engineered mouse models are ER-negative [32]. *PIK3CA* is by far the most frequently mutated gene in human luminal ER^+ breast cancers and several *Pik3ca*-mutant mouse models have been developed.

These models develop mammary tumors with mixed histology that do not resemble human luminal cancers, are variably positive for ER expression, and occur after a long latency and usually at incomplete penetrance [33–36]. This is in agreement with the spectrum of tumors and the pattern of ER expression that we have observed in our *Pik3ca*^{H1047R} knockin mouse model. Here on the other hand, we show that estrogen supplementation using slow-release 17β-estradiol pellets reduced tumor latency, increased penetrance, and resulted in exclusively ER$^+$ mammary tumors. Since tumors in our model arise long after the releasing action of the pellets has ceased, we hypothesize that supraphysiological levels of estrogen favor the initial steps of tumorigenesis in ER$^+$ cells, which are then transformed and give rise to ER + tumors before estrogen levels return to normal.

Several studies have indicated that inhibition of the PI3K pathway can increase the efficacy of antiestrogen therapy in ER$^+$ cells by enhancing ER function and dependence [15]. We too have observed an induction of ER in FR-1 cells after treatment with BYL719, although it did not render the cells responsive to fulvestrant. Mouse FR-2 and human MCF7-FR and T47D-FR cells that developed acquired resistance after long-term treated with fulvestrant were also minimally affected by the combined treatment. Interestingly, short- and long-term estrogen-deprived cells that retained ER expression but not those that lost it were sensitized to fulvestrant treatment after PI3K inhibition [14], indicating that PI3K inhibition may not be able to restore sensitivity to antiestrogen therapy when tumor growth is no longer dependent on estrogen.

Circumventing cell death is critical for tumor establishment and may underpin resistance to anticancer therapies [37]. Several studies have shown that inhibition of cell growth and induction of cell death are not always coupled when inhibiting the PI3K pathway [14]. This is in agreement with our observations in BYL719-treated *PIK3CA*- mutant human and mouse cells. The Bcl-2 family of proteins controls the mitochondrial pathway of apoptosis [38] and the PI3K pathway is a critical regulator of several Bcl-2 family members. Importantly, upregulation of Bcl-2 anti-apoptotic members [39] or downregulation of Bcl-2 pro-apoptotic members [40] have been previously suggested to drive resistance to kinase targeted therapies. Here we show that PI3Kα inhibition induces the pro-apoptotic Bcl-2 family member Bim, possibly by relieving the Akt mediated inhibition of FoxO3a, a well validated regulator of Bim expression in multiple cell systems [41, 42], but surprisingly fails to trigger apoptosis. We propose that this is due to the available pool of anti-apoptotic Bcl-2 family members and/or the induction of some of these proteins in a context-dependent manner, which can bind to and neutralize Bim. Interestingly, it has been previously shown that PI3K inhibition in certain PIK3CA and HER2 mutant breast cancer cells led in an ERK-dependent upregulation of BIM through P-REX1, which resulted in apoptosis in a fraction of the total population of these cells [43]. We too have observed a mild induction of apoptosis in response to treatment with BYL719 in some PIK3CA-mutant cells. However, addition of ABT263 was clearly effective at augmenting the apoptotic effects of BYL719 in all the PIK3CA-mutant cell lines that we tested (Fig. 5a).

Our knockdown experiments and the comparable efficacy of several BH3 mimetics against different Bcl-2 anti-apoptotic members suggest that Bim induction is critical for the activity of these compounds. Indeed, Bim can bind with high affinity to all anti-apoptotic BCL-2

family members [31, 44] and blockade of any of these proteins could relieve some portion of Bim inhibition. Of note, in a panel of over 500 human cancer cell lines high expression of Bim can predict sensitivity to ABT263 [45], which is in line with our observation that Bim induction correlated with increased efficacy of BH3 mimetics. Given the promising clinical activity of small molecule inhibitors targeting anti-apoptotic BCL-2 family members [46–49] and the fact that they were well tolerated these inhibitors could be suitable combinatorial partners with PI3K inhibition. In line with this, in the 315T PDX model, where AKT was found to be activated, triple therapy with ABT-737, a PI3K/mTOR inhibitor (PKI-587) and tamoxifen further augmented tumor response in vivo, when compared to ABT-737 and tamoxifen [50]. Moreover, our data show that combination of BYL719 and ABT263 was more effective at killing tumor cells than normal cells, and animals treated with these compounds showed no evidence of toxicity, suggesting that the toxicity profile may be manageable in people. Further studies are needed to assess their efficacy, as well as whether there will be a therapeutic window for such combinations in the clinic.

Materials and methods

Histological analysis and immunohistochemistry

Mouse mammary glands and tumors were fixed overnight in 10% buffered formalin and then dehydrated and embedded in paraffin. Paraffin blocks were sectioned at 5 μm and stained with hematoxylin and eosin. Immunophenotyping was performed with primary antibodies against CK5 (Covance, #AF 138), CK14 (Covance, #PRB-155P), CK18 (Abcam, #ab668) and ERα (Santa Cruz Biotechnology, sc-542). ERα and CK immunostaining was scored as follows: 0, no staining; 1 +, weak staining; 2+, focally strong (<15% of cells); 3+, strong in >15% of cells.

Immunofluorescence

Cells growing in 48-well plates were fixed for 15 min in cold 4% PFA in PBS. Cells were then washed twice (5 min) with cold PBS and incubated with blocking solution (5% horse serum and 1% Triton-X in PBS) for 1 h. Cells were then incubated O/N at 4 °C with the following primary antibodies prepared in blocking solution (CK5 1:50, CK14 1:300, CK18 1:300 and ERα 1:100 from Santa Cruz Bio-technology sc-543). The next day cells were washed twice (5 min) with cold PBS and then incubated with the following secondary antibodies prepared in blocking solution (Alexa Fluor 488 goat anti-rabbit from ThermoFisher Scientific #A-11034 at 1:1000 and Alexa Fluor 568 goat anti-mouse from ThermoFisher Scientific #A-11031 at 1:1000). Cells were then washed twice (5 min) with cold PBS and incubated with DAPI 1:10,000 in PBS for 10 min in the dark. Cells were then washed twice (5 min) with cold PBS and stored at 4 °C in the dark.

Proliferation and apoptosis assays

Experiments were carried out in 96-well plates in triplicates. A total of 1–3 × 10^3 cells per well were grown in the presence of 1 μM of BYL719 (Stand Up To Cancer) and ABT263 (Selleckchem), or 0.1 μM of fulvestrant (Selleckchem), ABT199 (Selleckchem), A1155463 (MedChem Express) and A1210477 (Selleckchem). Cells were then monitored for 3–4 days using the IncuCyte live cell imaging system (Essen BioScience, Ann Arbor, MI, USA),

which was placed in a cell culture incubator operated at 37 °C and 5% CO2. Cell confluence was determined using calculations derived from phase-contrast images. For measurement of cell death DRAQ7 (Cell Signaling # 7406) at 1.5 μM was included in the medium and apoptotic red counts were measured in IncuCyteTM FLR automated incubator microscope.

RNA interference

For Bim knockdown experiments MISSION® Lentiviral Transduction Particles against *Bcl2L11* (Clone ID: TRCN0000009692) and non-target control particles were purchased from Sigma-Aldrich and used according to the manufacturer's instructions. Briefly, ~10^5 cells were transduced with the viral particles at a MOI = 20 along with a final concentration of 8 μg/mL polybrene. Cells were selected with puromycin at 1 μg/mL for 7 days and then used immediately for signaling and cell growth analysis. For ERα knockdown experiments siRNA for the mouse *ESR1* was purchased from Qiagen. Cells were transfected using Lipofectamine (Invitrogen 11668–019) and knockdown was confirmed at 48 h. Scrambled siRNA was used as a control.

Statistics

Student *t* tests were used to test means between groups. Two-way ANOVA was used to test different treatment groups and Bonferroni's test to correct for multiple comparisons. Kaplan-Meier cumulative tumor-free survival curves were plotted and compared pairwise by the Mantel-Cox Log-rank test using GraphPad Prism 6 software. Mouse treatment studies were designed to use the minimum number of mice required to obtain informative results (meaning quantitative data amenable to statistical analysis) and sufficient material for subsequent studies. No specific statistical tests were used to predetermine the sample size; our previous experience with subcutaneous tumor models and pilot experiments provided guidance about the adequate number of mice that would provide significant results. Typically, we employed experimental cohorts of at least seven mice. No mice were excluded from the studies.

In vivo treatment study

Approximately 8-week-old female C57BL/6J mice were injected subcutaneously with 1 × 10^6 FR-1 cells in the right flank and 8-week-old female athymic nude mice, implanted with time release pellets (0.72 mg 17β-estradiol/60 days; Innovative Research of America), were injected with 3 × 10^6 MCF7-FR cells in the right flank. Females bearing tumor grafts were randomized in groups of 7–8 mice per group when tumor volumes reached ~100 mm^3. Animals were treated daily with BYL719 at 20 mg/kg (dissolved in 0.5% CMV) and/or ABT263 at 60 mg/kg (dissolved in Ethanol:PEG 400:Phosal 50 G at 10:30:60, respectively) by oral gavage. Tumor size was measured using calipers and tumor volume was calculated as follows: (long measurement × short measurement^2) × 0.5. Tumor sizes were recorded every three days over the course of the studies. Animal body weights were measured before and after the end of the treatment. Pharmacodynamic studies were performed on tumors after three days of treatment. Experiments involving mice were performed according to Mount Sinai School of Medicine Institutional Animal Care and Use Committee-approved protocols.

Supplementary Material

Refer to Web version on PubMed Central for supplementary material.

Acknowledgements

We would like to thank Stuart Aaronson and Jerry Chipuk for providing reagents and helpful discussions, Xi Sun for technical assistance and all members of the Parsons laboratory for critical reading of the manuscript. We also thank the Stand Up To Cancer (SU2C) PI3K Dream Team for providing BYL719. This work was supported by the Komen Foundation Scholar Award SAC110028 and NCI R01 CA129432 to R. Parsons. Additional support was given to E. Stratikopoulos from the Department of Defense Breast Cancer Research Program Era of Hope Award BC087596.

References

1. Dowsett M, Forbes JF, Bradley R, Ingle J, Aihara T, Bliss J, et al. Aromatase inhibitors versus tamoxifen in early breast cancer: patient-level meta-analysis of the randomised trials. Lancet. 2015;386:1341–52. [PubMed: 26211827]
2. Mouridsen H, Gershanovich M, Sun Y, Perez-Carrion R, Boni C, Monnier A, et al. Phase III study of letrozole versus tamoxifen as first-line therapy of advanced breast cancer in postmenopausal women: analysis of survival and update of efficacy from the International Letrozole Breast Cancer Group. J Clin Oncol. 2003;21:2101–9. [PubMed: 12775735]
3. Osborne CK, Schiff R. Mechanisms of endocrine resistance in breast cancer. Annu Rev Med. 2011;62:233–47. [PubMed: 20887199]
4. Robinson DR, Wu YM, Vats P, Su F, Lonigro RJ, Cao X, et al. Activating ESR1 mutations in hormone-resistant metastatic breast cancer. Nat Genet. 2013;45:1446–51. [PubMed: 24185510]
5. Toy W, Shen Y, Won H, Green B, Sakr RA, Will M, et al. ESR1 ligand-binding domain mutations in hormone-resistant breast cancer. Nat Genet. 2013;45:1439–45. [PubMed: 24185512]
6. Gutierrez MC, Detre S, Johnston S, Mohsin SK, Shou J, Allred DC, et al. Molecular changes in tamoxifen-resistant breast cancer: relationship between estrogen receptor, HER-2, and p38 mitogen-activated protein kinase. J Clin Oncol. 2005;23:2469–76. [PubMed: 15753463]
7. Koboldt DC, Fulton RS, McLellan MD, Schmidt H, Kalicki-Veizer J, McMichael JF. et al.Comprehensive molecular portraits of human breast tumours.Nature.2012;490:61–70. [PubMed: 23000897]
8. Yu M, Bardia A, Aceto N, Bersani F, Madden MW, Donaldson MC, et al. Cancer therapy. Ex vivo culture of circulating breast tumor cells for individualized testing of drug susceptibility. Science. 2014;345:216–20. [PubMed: 25013076]
9. Saal LH, Holm K, Maurer M, Memeo L, Su T, Wang X, et al. PIK3CA mutations correlate with hormone receptors, node metastasis, and ERBB2, and are mutually exclusive with PTEN loss in human breast carcinoma. Cancer Res. 2005;65:2554–9. [PubMed: 15805248]
10. Sabnis G, Goloubeva O, Jelovac D, Schayowitz A, Brodie A. Inhibition of the phosphatidylinositol 3-kinase/Akt pathway improves response of long-term estrogen-deprived breast cancer xenografts to antiestrogens. Clin Cancer Res. 2007;13:2751–7. [PubMed: 17473209]
11. Crowder RJ, Phommaly C, Tao Y, Hoog J, Luo J, Perou CM, et al. PIK3CA and PIK3CB inhibition produce synthetic lethality when combined with estrogen deprivation in estrogen receptor-positive breast cancer. Cancer Res. 2009;69:3955–62. [PubMed: 19366795]
12. Miller TW, Hennessy BT, Gonzalez-Angulo AM, Fox EM, Mills GB, Chen H, et al. Hyperactivation of phosphatidylinositol-3 kinase promotes escape from hormone dependence in estrogen receptor-positive human breast cancer. J Clin Invest. 2010;120:2406–13. [PubMed: 20530877]
13. Creighton CJ, Fu X, Hennessy BT, Casa AJ, Zhang Y, Gonzalez-Angulo AM, et al. Proteomic and transcriptomic profiling reveals a link between the PI3K pathway and lower estrogen-receptor (ER) levels and activity in ER+ breast cancer. Breast Cancer Res. 2010;12:R40. [PubMed: 20569503]

14. Sanchez CG, Ma CX, Crowder RJ, Guintoli T, Phommaly C, Gao F, et al. Preclinical modeling of combined phosphatidylinositol-3-kinase inhibition with endocrine therapy for estrogen receptor-positive breast cancer. Breast Cancer Res. 2011;13:R21. [PubMed: 21362200]
15. Bosch A, Li Z, Bergamaschi A, Ellis H, Toska E, Prat A, et al. PI3K inhibition results in enhanced estrogen receptor function and dependence in hormone receptor-positive breast cancer. Sci Transl Med. 2015;7:283ra51.
16. Toska E, Osmanbeyoglu HU, Castel P, Chan C, Hendrickson RC, Elkabets M, et al. PI3K pathway regulates ER-dependent transcription in breast cancer through the epigenetic regulator KMT2D. Science. 2017;355:1324–30. [PubMed: 28336670]
17. Bachelot T, Bourgier C, Cropet C, Ray-Coquard I, Ferrero JM, Freyer G, et al. Randomized phase II trial of everolimus in combination with tamoxifen in patients with hormone receptor-positive, human epidermal growth factor receptor 2-negative metastatic breast cancer with prior exposure to aromatase inhibitors: a GINECO study. J Clin Oncol. 2012;30:2718–24. [PubMed: 22565002]
18. Baselga J, Campone M, Piccart M, Burris HA 3rd, Rugo HS, Sahmoud T, et al. Everolimus in postmenopausal hormone-receptor-positive advanced breast cancer. N Engl J Med. 2012;366:520–9. [PubMed: 22149876]
19. Mayer IA, Arteaga CL. The PI3K/AKT pathway as a target for cancer treatment. Annu Rev Med. 2016;67:11–28. [PubMed: 26473415]
20. Krop IE, Mayer IA, Ganju V, Dickler M, Johnston S, Morales S, et al. Pictilisib for oestrogen receptor-positive, aromatase inhibitor-resistant, advanced or metastatic breast cancer (FERGI): a randomised, double-blind, placebo-controlled, phase 2 trial. Lancet Oncol. 2016;17:811–21. [PubMed: 27155741]
21. Baselga J, Im S-A, Iwata H, Clemons M, Ito Y, Awada A, et al. Abstract S6–01: PIK3CA status in circulating tumor DNA (ctDNA) predicts efficacy of buparlisib (BUP) plus fulvestrant (FULV) in postmenopausal women with endocrine-resistant HR+/HER2-advanced breast cancer (BC): first results from the randomized, phase III BELLE-2 trial. Cancer Res. 2016;76:S6–01–S6-.
22. Juric D, Burris H, Schuler M, Schellens J, Berlin J, Seggewiß-Bernhardt R, et al. 451PDphase I study of the pi3kα inhibitor BYL719, as a single agent in patients with advanced solid tumors (AST). Ann Oncol. 2014;25:iv150–iv.
23. Shah PD, Modi S, Datko FM, Moynahan ME, Zamora S, D'Andrea G, et al. Phase I trial of daily PI3Kα inhibitor BYL719 plus letrozole (L) or exemestane (E) for patients (pts) with hormone receptor-positive (HR+) metastatic breast cancer (MBC). J Clin Oncol. 2014;32:2605-.
24. Mayer IA, Abramson VG, Formisano L, Balko JM, Estrada MV, Sanders ME, et al. A phase Ib study of alpelisib (BYL719), a PI3Kalpha-specific inhibitor, with letrozole in ER+/HER2-metastatic breast cancer. Clin Cancer Res. 2017;23:26–34. [PubMed: 27126994]
25. Ndubaku CO, Heffron TP, Staben ST, Baumgardner M, Blaquiere N, Bradley E, et al. Discovery of 2-{3-[2-(1-isopropyl-3-methyl-1H-1,2–4-triazol-5-yl)-5,6-dihydrobenzo[f]imidazo[1, 2-d][1,4] oxazepin-9-yl]-1H-pyrazol-1-yl}−2-methylpropanamide (GDC-0032): a beta-sparing phosphoinositide 3-kinase inhibitor with high unbound exposure and robust in vivo antitumor activity. J Med Chem. 2013;56:4597–610. [PubMed: 23662903]
26. Saura C, Sachdev J, Patel MR, Cervantes A, Juric D, Infante JR, et al. Abstract PD5–2: Ph1b study of the PI3K inhibitor taselisib (GDC-0032) in combination with letrozole in patients with hormone receptor-positive advanced breast cancer. Cancer Res. 2015;75:PD5–2–PD5–2.
27. Baird RD, Rossum AV, Oliveira M, Beelen K, Garcia-Corbacho J, Mandjes IAM, et al. POSEIDON trial phase 1b results: safety and preliminary efficacy of the isoform selective PI3K inhibitor taselisib (GDC-0032) combined with tamoxifen in hormone receptor (HR) positive, HER2-negative metastatic breast cancer (MBC) patients (pts) - including response monitoring by plasma circulating tumor (ct) DNA. J Clin Oncol. 2016;34:2520-.
28. Stratikopoulos EE, Dendy M, Szabolcs M, Khaykin AJ, Lefebvre C, Zhou MM, et al. Kinase and BET inhibitors together clamp inhibition of PI3K signaling and overcome resistance to therapy. Cancer Cell. 2015;27:837–51. [PubMed: 26058079]
29. Ludwig T, Fisher P, Murty V, Efstratiadis A. Development of mammary adenocarcinomas by tissue-specific knockout of Brca2 in mice. Oncogene. 2001;20:3937–48. [PubMed: 11494122]

30. Putcha GV, Moulder KL, Golden JP, Bouillet P, Adams JA, Strasser A, et al. Induction of BIM, a proapoptotic BH3-only BCL-2 family member, is critical for neuronal apoptosis. Neuron. 2001;29:615–28. [PubMed: 11301022]

31. Chen L, Willis SN, Wei A, Smith BJ, Fletcher JI, Hinds MG, et al. Differential targeting of prosurvival Bcl-2 proteins by their BH3-only ligands allows complementary apoptotic function. Mol Cell. 2005;17:393–403. [PubMed: 15694340]

32. Mohibi S, Mirza S, Band H, Band V. Mouse models of estrogen receptor-positive breast cancer. J Carcinog. 2011;10:35. [PubMed: 22279420]

33. Adams JR, Xu K, Liu JC, Agamez NM, Loch AJ, Wong RG, et al. Cooperation between Pik3ca and p53 mutations in mouse mammary tumor formation. Cancer Res. 2011;71:2706–17. [PubMed: 21324922]

34. Meyer DS, Brinkhaus H, Muller U, Muller M, Cardiff RD, Bentires-Alj M. Luminal expression of PIK3CA mutant H1047R in the mammary gland induces heterogeneous tumors. Cancer Res. 2011;71:4344–51. [PubMed: 21482677]

35. Tikoo A, Roh V, Montgomery KG, Ivetac I, Waring P, Pelzer R. Physiological levels of Pik3ca(H1047R) mutation in the mouse mammary gland results in ductal hyperplasia and formation of ERalpha-positive tumors. PLoS One. 2012;7:e36924. [PubMed: 22666336]

36. Yuan W, Stawiski E, Janakiraman V, Chan E, Durinck S, Edgar KA, et al. Conditional activation of Pik3ca(H1047R) in a knock-in mouse model promotes mammary tumorigenesis and emergence of mutations. Oncogene. 2013;32:318–26. [PubMed: 22370636]

37. Hanahan D, Weinberg RA. Hallmarks of cancer: the next generation. Cell. 2011;144:646–74. [PubMed: 21376230]

38. Shamas-Din A, Kale J, Leber B, Andrews DW. Mechanisms of action of Bcl-2 family proteins. Cold Spring Harb Perspect Biol. 2013;5:a008714. [PubMed: 23545417]

39. Muranen T, Selfors LM, Worster DT, Iwanicki MP, Song L, Morales FC, et al. Inhibition of PI3K/mTOR leads to adaptive resistance in matrix-attached cancer cells. Cancer Cell. 2012;21:227–39. [PubMed: 22340595]

40. Hata AN, Yeo A, Faber AC, Lifshits E, Chen Z, Cheng KA, et al. Failure to induce apoptosis via BCL-2 family proteins underlies lack of efficacy of combined MEK and PI3K inhibitors for KRAS-mutant lung cancers. Cancer Res. 2014;74:3146–56. [PubMed: 24675361]

41. Essafi A, Fernandez de Mattos S, Hassen YA, Soeiro I, Mufti GJ, Thomas NS, et al. Direct transcriptional regulation of Bim by FoxO3a mediates STI571-induced apoptosis in Bcr-Abl-expressing cells. Oncogene. 2005;24:2317–29. [PubMed: 15688014]

42. Sunters A, Fernandez de Mattos S, Stahl M, Brosens JJ, Zoum-poulidou G, Saunders CA, et al. FoxO3a transcriptional regulation of Bim controls apoptosis in paclitaxel-treated breast cancer cell lines. J Biol Chem. 2003;278:49795–805. [PubMed: 14527951]

43. Ebi H, Costa C, Faber AC, Nishtala M, Kotani H, Juric D, et al. PI3K regulates MEK/ERK signaling in breast cancer via the Rac-GEF, P-Rex1. Proc Natl Acad Sci USA. 2013;110:21124–9. [PubMed: 24327733]

44. O'Connor L, Strasser A, O'Reilly LA, Hausmann G, Adams JM, Cory S, et al. Bim: a novel member of the Bcl-2 family that promotes apoptosis. EMBO J. 1998;17:384–95. [PubMed: 9430630]

45. Faber AC, Farago AF, Costa C, Dastur A, Gomez-Caraballo M, Robbins R, et al. Assessment of ABT-263 activity across a cancer cell line collection leads to a potent combination therapy for small-cell lung cancer. Proc Natl Acad Sci USA. 2015;112: E1288–1296. [PubMed: 25737542]

46. Wilson WH, O'Connor OA, Czuczman MS, LaCasce AS, Ger-ecitano JF, Leonard JP, et al. Navitoclax, a targeted high-affinity inhibitor of BCL-2, in lymphoid malignancies: a phase 1 dose-escalation study of safety, pharmacokinetics, pharmacodynamics, and antitumour activity. Lancet Oncol. 2010;11:1149–59. [PubMed: 21094089]

47. Gandhi L, Camidge DR, Ribeiro de Oliveira M, Bonomi P, Gandara D, Khaira D, et al. Phase I study of navitoclax (ABT-263), a novel Bcl-2 family inhibitor, in patients with small-cell lung cancer and other solid tumors. J Clin Oncol. 2011;29:909–16. [PubMed: 21282543]

48. Roberts AW, Seymour JF, Brown JR, Wierda WG, Kipps TJ, Khaw SL, et al. Substantial susceptibility of chronic lymphocytic leukemia to BCL2 inhibition: results of a phase I study of

navitoclax in patients with relapsed or refractory disease. J Clin Oncol. 2012;30:488–96. [PubMed: 22184378]

49. Roberts AW, Davids MS, Pagel JM, Kahl BS, Puvvada SD, Gerecitano JF, et al. Targeting BCL2 with venetoclax in relapsed chronic lymphocytic leukemia. N Engl J Med. 2016;374:311–22. [PubMed: 26639348]
50. Vaillant F, Merino D, Lee L, Breslin K, Pal B, Ritchie ME, et al. Targeting BCL-2 with the BH3 mimetic ABT-199 in estrogen receptor-positive breast cancer. Cancer Cell. 2013;24:120–9. [PubMed: 23845444]

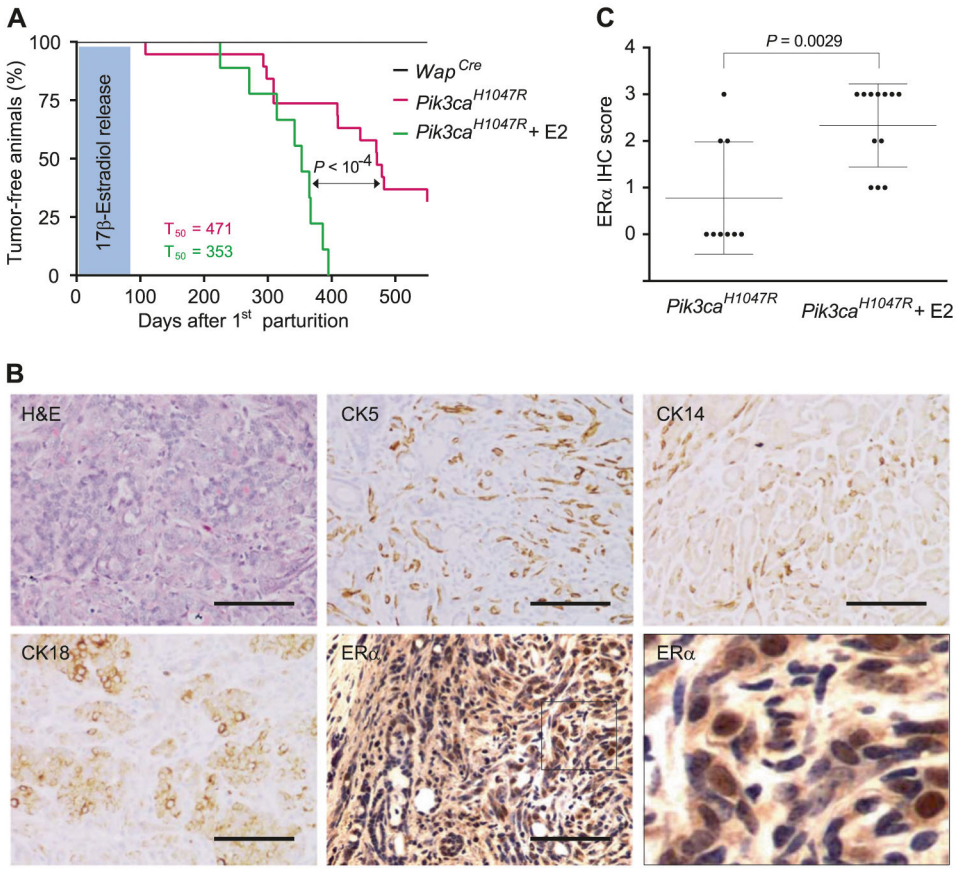

Fig. 1.

Estrogen supplementation enhances the emergence of ER$^+$ mouse mammary tumors driven by *Pik3ca*^{H1047R}. **a** Kaplan-Meier plots of tumor occurrence detected by palpation in control *Wap*^{Cre} ($n = 12$) mice and in two cohorts of *Pik3ca*^{H1047R} female mice, with (*H1047R* + E2; $n = 9$) or without (*H1047R;* $n = 19$) the presence of estrogen-releasing pellets. *P* value was calculated using the Mantel-Cox Log-rank test. **b** Representative sections showing H&E staining and CK5, CK14, CK18, and ERα immunostaining in an estrogen-treated adenocarcinoma that was used to derive the FR-1 tumor cell line. Scale bars, 50 μm. **c** ER immunostaining score of mammary tumors in the *H1047R* and *H1047R* + E2 cohorts. Each dot represents a different tumor. *P* value was calculated using a two-tailed Student's *t* test

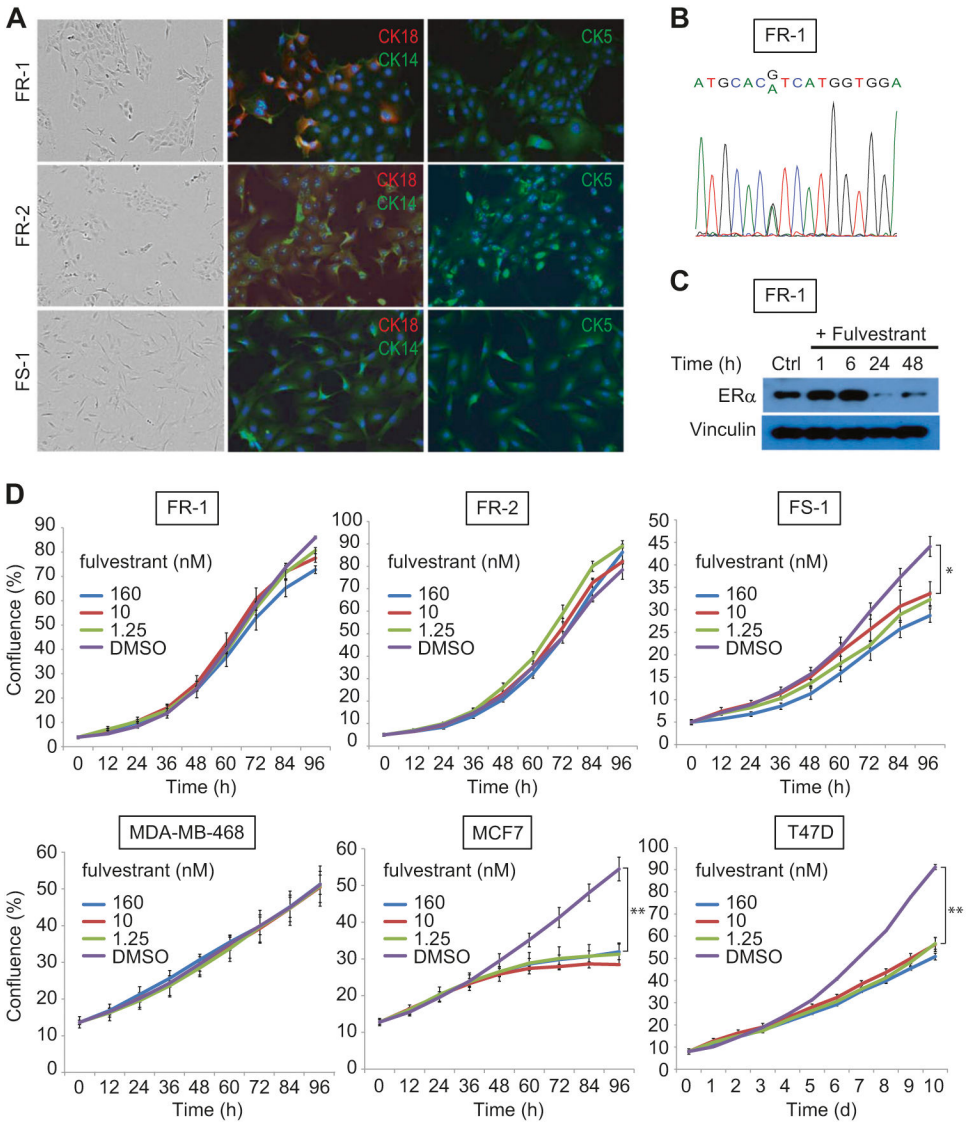

Fig. 2.

Mouse *ER*$^{+}$*/Pik3ca*^{H1047R} cells vary in their response to hormonal therapies. **a** Phase-contrast images and immunofluorescence for CKs 5, 14, and 18 in mouse cells. **b** mRNA was isolated from FR-1 cells and primers flanking the H1047R *Pik3ca* mutation hotspot were used to PCR amplify and sequence the region of interest. **c** Western blot analysis in FR-1 cells treated with fulvestrant for the indicated time points. **d** Effects of fulvestrant on cell growth. Results are shown as percent confluence and represent the average ± SD of three technical replicates. *$P < 0.001$, **$P < 0.0001$. *P* value was calculated using two-way ANOVA

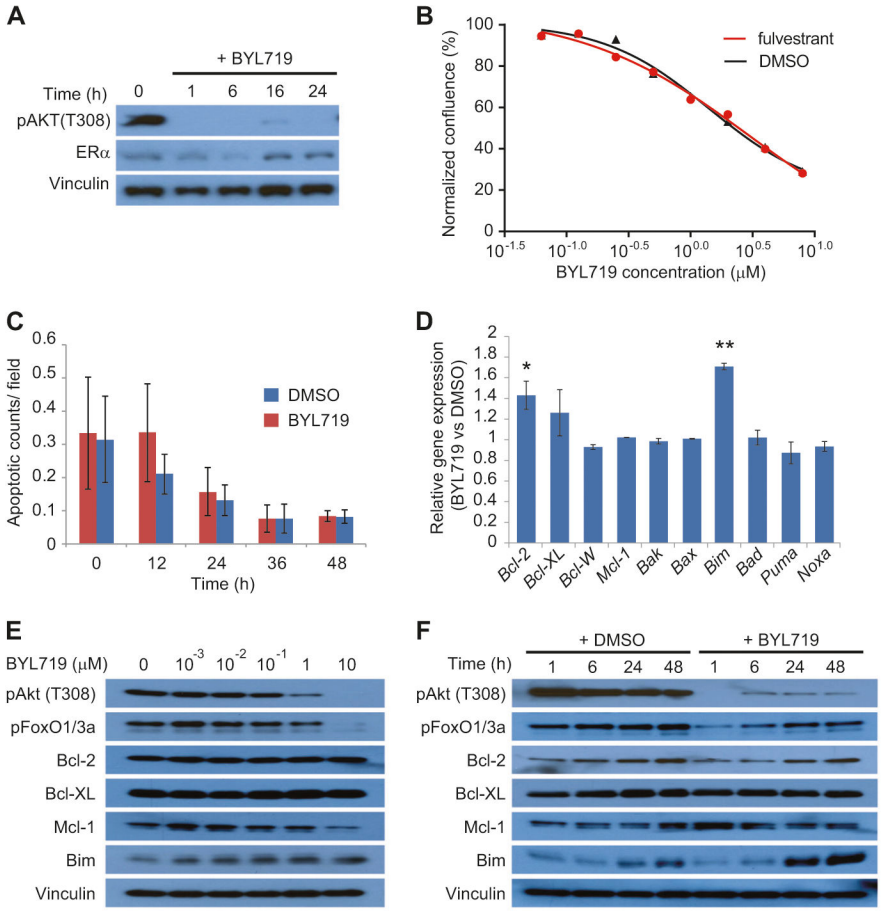

Fig. 3.

PI3Kα inhibition fails to induce cell death despite Bim upregulation in FR-1 cells. **a** Cells were treated with 1 μM BYL719 for the indicated time points and protein levels were analyzed through western blot. **b** Cells were treated with the indicated concentrations of BYL719 plus either DMSO or 100 nM of fulvestrant and growth was measured after 2 days of treatment. Results represent the average of three replicates. **c** Cells were treated with either DMSO or 1 μM BYL719 in the presence of 1.5 μM DRAQ7 for the indicated time points. Apoptotic red counts were calculated using the IncuCyte FLR object counting. Data were normalized to confluence and represent the average ± SD of three technical replicates. **d** Quantitative RT-PCR for the indicated genes was performed using mRNA from cells that were treated with either DMSO or 1 μM BYL719 for 6h. Results were normalized to actin and error bars indicate ± SD of three technical replicates. Two-tailed Student's *t* test was performed to compare DMSO versus BYL719. **P*<0.05, ***P*<0.001. **e** Cells were treated with the indicated concentrations of BYL719 for 24 h and protein levels were analyzed through immunoblot. **f** Cells were treated with either DMSO or 1 μM BYL719 for the indicated time points and protein levels were analyzed through immunoblot

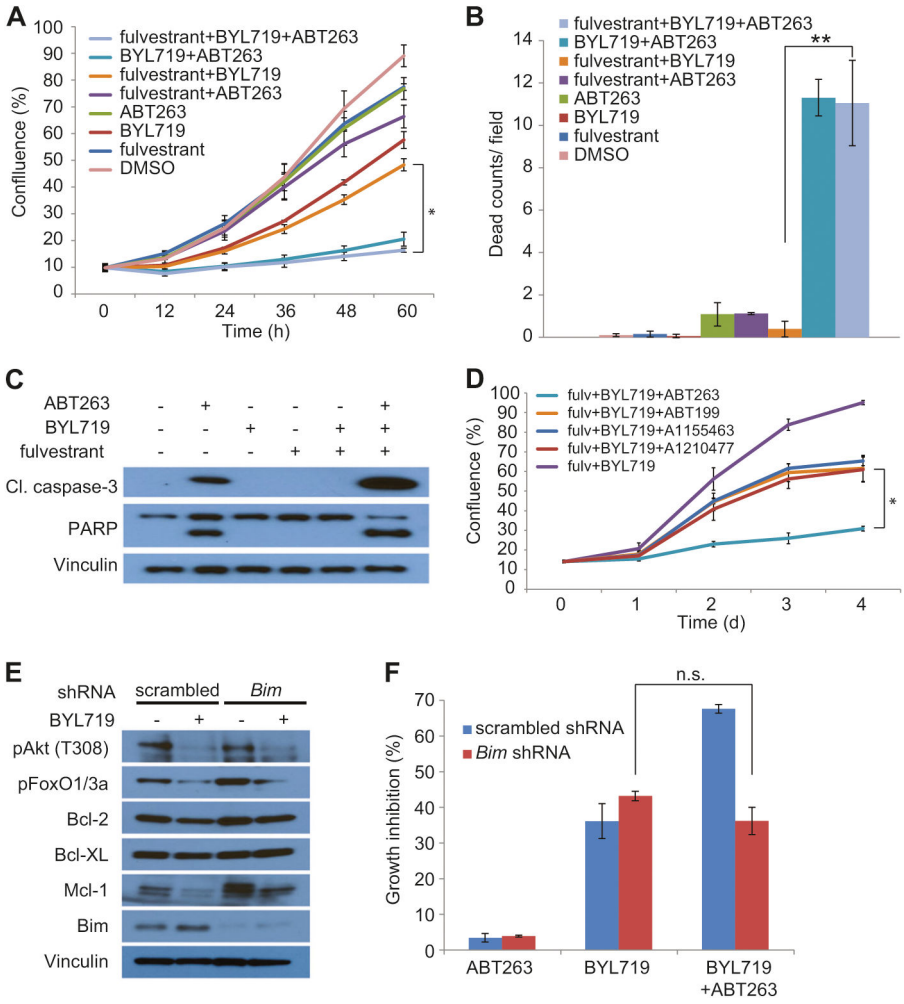

Fig. 4.

Combination of BH3 mimetics and PI3Kα inhibition induces cell death. **a** FR-1 cells were treated with DMSO, 1 μM BYL719, 1 μM ABT263, 100 nM fulvestrant or their combinations for the indicated time points and cell growth was calculated using calculations derived from phase-contrast images. Results represent the average ± SD of three technical replicates. *P <0.0001. P value was calculated using two-way ANOVA. **b** FR-1 cells were treated as before and apoptotic red counts were calculated after 2 days of treatment. Results represent the average ±SD of three technical replicates. **P <0.001. P value was calculated using an unpaired two-tailed Student's t-test. **c** FR-1 cells were treated as before for 24 h and protein levels were analyzed through immunoblot. **d** FR-1 cells were treated with 1 μM BYL719 and 100 nM fulvestrant plus 1 μM ABT263 or 0.1 μM ABT199, A1155463, or A1210477 for the indicated time points and cell growth was calculated as before. Results represent the average ± SD of three technical replicates. *P <0.0001. P value was calculated using two-way ANOVA. **e** FR-1 cells were transduced with either a scrambled or an anti-*Bim* shRNA and indicated protein levels were analyzed through immunoblot 24 h after treatment with either 1 μM BYL719 or DMSO. f Growth inhibition data were derived from calculations of confluence based on phase-contrast images of FR-1 cells transduced with

either a scrambled or an anti-*Bim* shRNA and treated with either 1 μM BYL719 or DMSO after 3 days of treatment. Results represent the average ± SD of three technical replicates

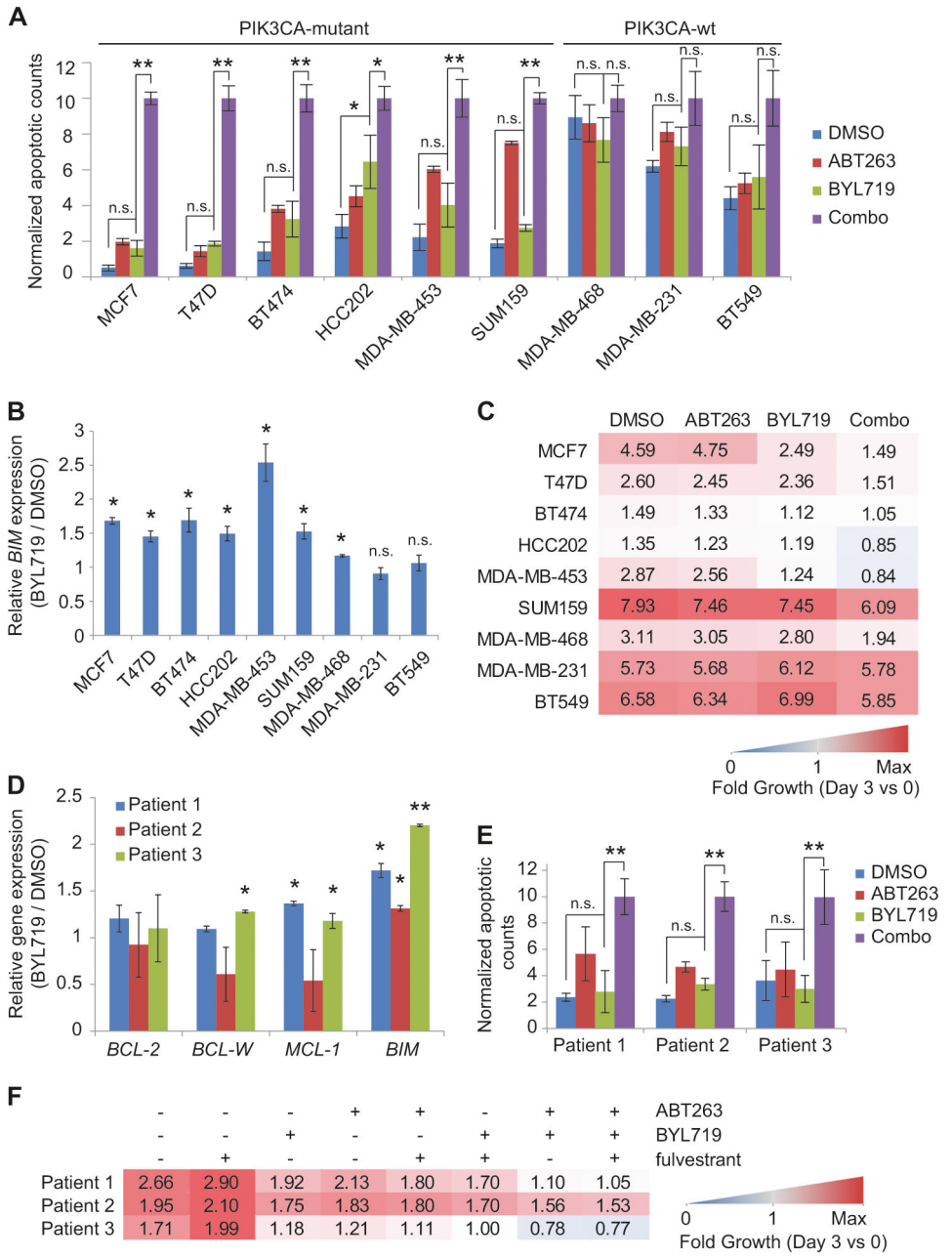

Fig. 5.

ABT263 enhances the efficacy of PI3Kα inhibition in PIK3CA-mutant cells. **a** Human breast cancer cells were treated with DMSO, 1 μM BYL719, 1 μM ABT263 or their combination. Apoptotic red counts were calculated after 2 days of treatment. Results represent the average ± SD of three technical replicates. **P* < 0.05, ***P* <0.001. Adjusted *P* value was calculated using two-way ANOVA and Bonferroni's test for multiple comparisons. **b** Expression of indicated genes in cells treated for 6 h with 1 μM BYL719 or DMSO. Results were normalized to actin and error bars indicate ± SD of three technical replicates. **P* < 0.05. *P* value was calculated using a two-tailed Student's *t* test. **c** Cells were treated as above and cell growth is presented as percent confluence. Results represent the

average of three technical replicates. Fold growth <1 represents reduction of cell confluence at the end of the experiment. **d-f** Same as **a-c** using early passage tumor-derived breast epithelial cells from three different patients. *P <0.05, **P <0.001. Adjusted P value was calculated using two-way ANOVA and Bonferroni's test for multiple comparisons. n. s non-significant

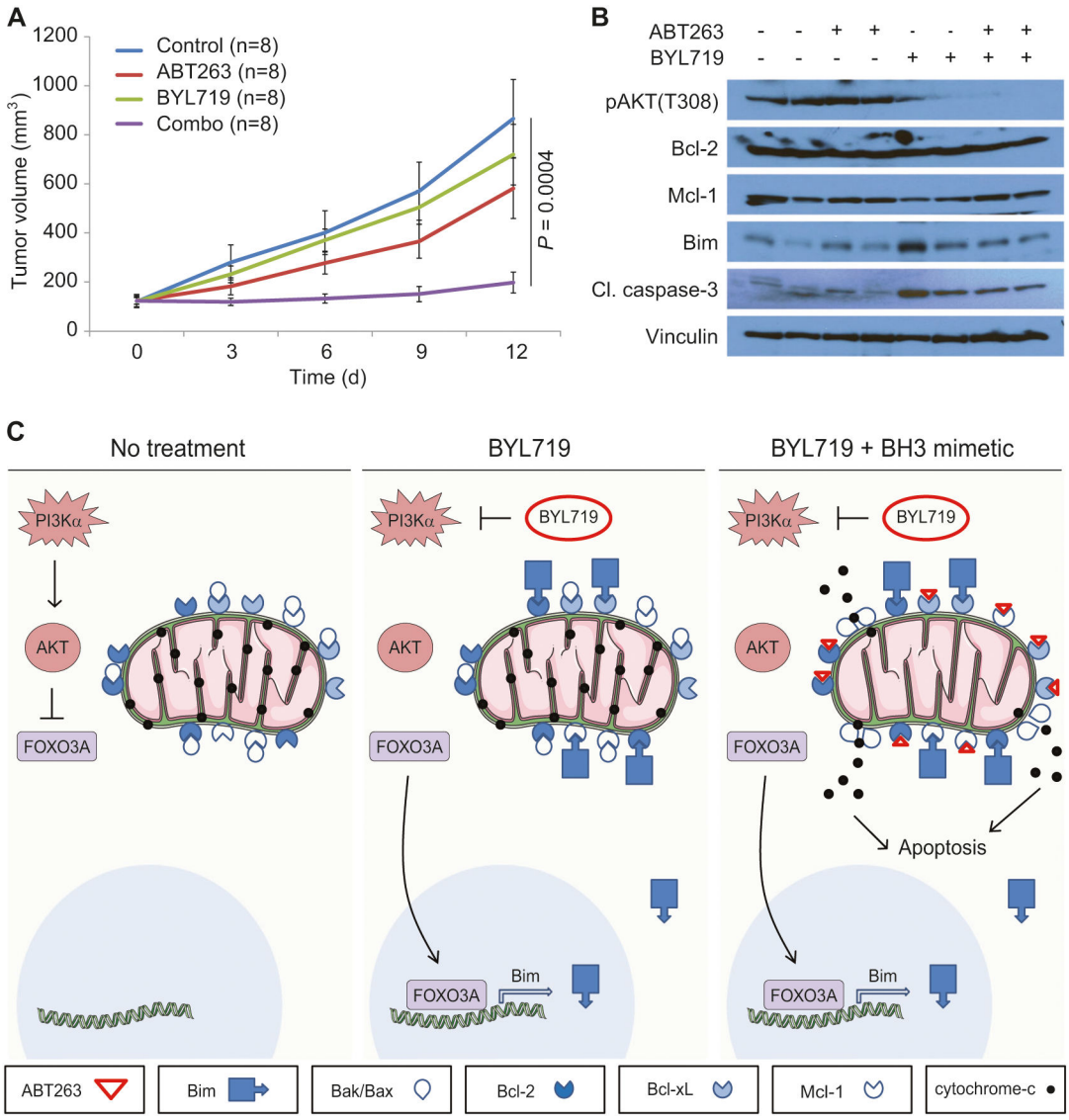

Fig. 6.

ABT263 enhances the efficacy of BYL719 in vivo. **a** Tumor growth data from FR-1 allografts treated with the indicated compounds or vehicle control for 12 days. Number of mice per arm (*n*) is shown in parentheses. **b** FR-1 allografts were treated for 3 days with the indicated compound, at which point tumors were harvested and snap frozen. Levels of indicated proteins were assessed through western blot for two different animals per treatment group. **c** Schematic representation of cell death induction model with the combined use of PI3Kα inhibition and BH3 mimetics